INVESTIGATION OF SATURATION TEMPERATURE IN SOLAR POND FOR DIFFERENT SIZES

by

Haci SOGUKPINAR [a] ***and Ismail BOZKURT*** [b*]

[a] Department of Electric and Energy, Vocational School, University of Adiyaman, Adiyaman, Turkey
[b] Department of Mechanical Engineering, Faculty of Engineering, University of Adiyaman, Adiyaman, Turkey

Original scientific paper
https://doi.org/10.2298/TSCI181222161S

This paper deals with the modelling of solar ponds for different sizes to calculate saturation time and temperature by using discrete ordinates method. The modeled solar pond is a subsoil type and aimed to minimize the heat losses by isolating side wall and ground with foam with the thickness of 10 cm in all cases. In the model, upper convective zone is 10 cm deep and non-convective zone consists of five layer and each layer is 10 cm deep and storage zone depth ranges from 40-400 cm. Therefore, the solar pond totally consists of seven layers. The saturation temperature was found to be about 322 K for 12 different solar pond. For a depth of 40 cm, the equilibrium temperature was reached in 1000 hours, 1300 hours for 60 cm, 1400 hours for 80 cm, 1500 hours for 100 cm, 1600 hours for 120 cm, 1750 hours for 1140 cm, 1800 hours for 180 cm, 2700 hours for 200 cm, 1800 hours for 250 cm, 3400 hours for 300 cm, and 6000 hours have passed for 400 cm. As the depth increases, time to reach to the equilibrium temperature increases but increment amount of water and time to reach equilibrium temperature shows a proportional increase. At the same time we calculated that, when we increase the width of the pond by keeping the depth constant, the saturation temperature and the time did not changed for the seven different cases.

Key words: *solar energy, solar pond, saturation time and temperature*

Introduction

The importance of energy demand has been increasing with the reducing energy sources and increasing prices. Furthermore, the global warming effects our lives adversely in each passing day. In the other hand, in order to reduce external dependence for energy demand, it is necessary to generate from domestic sources. In this case, RES are an alternative way to conventional energy sources. There are many RES such as solar, wind, geothermal, *etc.* Solar energy is the most important of these energy resources. Solar energy systems are used in many purposes such as direct electricity generation, heat storage, heating and cooling systems. The development of solar systems covering part of the thermal energy required in the residential sector is a viable option for reducing fossil fuel use and might solve an important part of the energy problems [1].

Solar ponds are one of the systems in which solar energy is stored as heat. This system is very useful for medium temperature applications with simple installation, and also

* Corresponding author, e-mail: ibozkurt@adiyaman.edu.tr

low installation and low maintenance costs. This system can be used for electricity generation, heating of greenhouses and swimming ponds, distillation of salt water, and drying food, *etc.* Many experimental and theoretical studies on the performance of solar ponds have been carried out. Various transparent cover systems, reflective surfaces, different insulation parameters, integrated with systems, *etc.* were proposed to increase the thermal performance of the solar pond [2-5]. Bozkurt *et al.* [6] have studied on increasing the performance of the solar pond. Solar pond integrated with collector system were constructed to calculate the solar pond efficiencies according to the number of collectors. The effect of the transparent covers were investigated to increase the light transmission through the transparent cover and also decrease the heat losses to air from the upper zone of the pond [7]. The effect of the sunny area ratios were studied on thermal efficiency of model solar pond for different cases [8]. An experimental magnesium chloride with saturated solar pond was constructed for experimental investigations, and its performance was investigated and evaluated through energy and exergy efficiencies [9]. Ganguly *et al.* [10] investigated the thermal performance of the pond with the method of adding heat to a salt gradient solar pond from evacuated tube solar collectors. Heat addition from the external source enhances the thermal performance of solar pond in terms of heat recovery and thermal efficiency with certain constraints. Sayer *et al.* [11] investigated the influence of varying the thicknesses of the zones on temperatures change. The temperature of heat storage zone (HSZ) has a considerable impact on the optimal thicknesses of the upper convective zone (UCZ) and the non-convective zone. Akrour *et al.* [12] investigated the effect of thermodiffusion on the stability of a gradient layer to clarify the mechanisms of fluid dynamics and the processes in a salinity gradient solar pond. Alcaraz *et al.* [13] evaluated a 500 m^2 industrial solar pond in Granada, Spain, during an event of extreme weather conditions of snowfall during the winter. Sayer *et al.* [14] studied the feasibility of the gel pond and compared salt gradient solar pond with gel solar pond. Montala *et al.* [15] developed a methodology to study the stability of the industrial solar pond. Two different methodologies based on the stratification principle were adapted and used to determine the stability of the solar pond.

Many studies have been performed about solar ponds with different sizes and features. For all that, there have not been any investigations on the modelling of solar ponds for different sizes to calculated saturation time and temperature. This was in fact the key motivation behind the present work. The solar pond temperature reaches a certain maximum temperature value depending on the solar energy. After this saturation temperature, the temperature becomes stable and no increase is observed. By determining the maximum saturation temperature and time of the solar pond, the performance of the pond can be increased by withdrawing heat from the pond. In this work, 12 solar ponds with different depth were simulated. The saturation time and temperature of the solar ponds were investigated for different dimensions. At the same time, seven different solar ponds were modeled to determine the saturation temperature and the time duration when we increase the width of the pond by keeping the depth constant.

Modelling of solar pond and its structure

Solar ponds collect solar energy and are capable of storing heat energy for a long time. Solar ponds usually consist of three zones. The bottom of the solar pond is called HSZ. This zone was formed with high density salty water. The second zone is called non-convective zone (NCZ). This zone consists of several layers, where density decreases from HSZ to the surface of the pond. The surface zone of the solar pond is called UCZ [16].

The interaction of solar radiation with the solar pond continues from the surface of the UCZ to the HSZ. Some of the solar radiation coming to the surface is absorbed by the salty layers and some is scattered in different directions. The vast majority of the remaining part transmitted to a substrate without being absorbed. In addition, some of the absorbed light is emitted around by means of radiation. Interaction continues in the same way as it passes from each upper layer to a lower layer. Radiation is another heat transfer method that should be consider in addition conduction and convection. Polished materials has emissivity less than 0.1 whereas other materials such as dark surface, plastic, skin, paper, and ceramic have an emissivity more than 0.8. Let $I(\Omega)$ represent radiative intensity incident on the surface and three different kind of interaction are expected to observe. These are absorption, emission and scattering. The medium absorb a part of radiation depend on absorption coefficient, κ, and the medium emit some part of radiation in all direction. Part of incoming radiation is scattered in other directions. The general incoming solar radiation transfer equation can be represented [17, 18]:

$$\Omega \nabla I(\Omega) = \kappa I_b(T) - \beta I(\Omega) + \frac{\sigma_s}{4\pi}\int_0^4 I(\Omega')\phi(\Omega',)\Omega \mathrm{d}\Omega' \tag{1}$$

where $I(\Omega)$ is the radiative intensity at a given position, κ, – the absorption, β – the extinction, and σ_s – the scattering coefficients, $I_b(T)$ – the blackbody radiative intensity, $\varphi(\Omega', \Omega)$ – the scattering phase function, σ – the Stefan-Boltzmann constant, and T – the temperature. Interaction of incident radiation with solar pond was simulated by solving eq. (1) for each mesh point. Heat lost in the side wall and ground surface mainly happened by conduction. Heat transfer equation in these part can represented [19]:

$$\rho C_P\left(\frac{\partial T}{\partial t} + \vec{\mathrm{u}}_{\mathrm{trans}}\nabla T\right) + \nabla(\vec{\mathrm{q}} + \vec{\mathrm{q}}_{\mathrm{r}}) = -\alpha T : \frac{\mathrm{d}\mathbf{S}}{\mathrm{d}t} + Q \tag{2}$$

where C_p is the specific heat capacity, $\vec{\mathrm{u}}_{\mathrm{trans}}$ – the velocity vector of translational motion, $\mathbf{S}$ – the second Piola-Kirchhoff stress tensor. On the surface, heat lost mainly happened by natural-convection. The convective heat flux on the open surface is proportional to the temperature difference between UCZ zone and the air. Mathematical representation of convective heat flux is described [20]:

$$-\vec{\mathrm{n}} \cdot \vec{\mathrm{q}} = h(T_{\mathrm{ext}} - T) \tag{3}$$

where h is a heat transfer coefficient and T_{ext} – the temperature of the external fluid far from the boundary. The h is depend on material properties, surface temperature and also fluid-flow rate. For radiation discretization method S4 type discrete ordinate method was employed. Some other heat transfer constant were used from COMSOL library. The modeled solar pond is a subsoil type and it was aimed to minimize the heat losses by isolating side wall and ground with foam with the thickness of 10 cm in all cases. In the model, UCZ is 10 cm deep and NCZ consists of five layer and each layer is 10 cm deep. Therefore, the solar pond totally consists of seven layers. The model solar pond was simulated with the help of the commercial COMSOL program by using discrete ordinates method. For the current study direct solver PARDISO with nested dissection multithreaded preordering algorithm was used. The mesh distribution for the model is shown in fig. 1. Mesh density was increased at the point where temperatures were calculated. For all models, the most consistent results were calculated when extremely fine mesh type was chosen. The way the solar radiation incident to the surface of the pond was modeled as which is coming from both upper corners. The interaction of solar radiation with the pond was modeled and is shown in fig. 2. As seen, the rays are absorbed while passing through the layers and

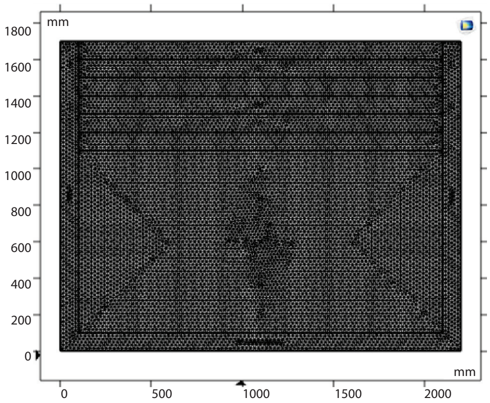

Figure 1. Mesh distribution for the modeled solar pond

the intensity is reduced. The heat flux of the surfaces and inner zones of solar pond is shown in fig. 3. Computational conditions are given in tab. 1 for this model.

Results and discussions

In this study, time to reach equilibrium temperature was investigated by changing the depth of the HSZ. Size of UCZ and NCZ were kept constant. Numerical calculation was tested in the preliminary calculation for varied mesh distribution and compared with an experimental study which was conducted for the Mediterranean region [21, 22]. The comparison between this calculation and experiment show good agreement and results are found to be very well matched for this model. Meteorology has been measuring the solar radiation since 1987 and the arithmetic average of these data was used, tab. 2. In numerical calculations, solar radiation and temperature data for ADANA were utilized for consistency check. Air and soil temperatures were applied by taking the annual arithmetic average of the meteorological temperature data. The heat losses from the side wall and bottom surface mainly happened through the conduction path but

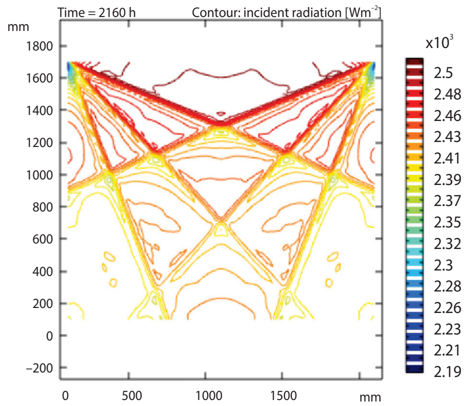

Figure 2. Rate of change of incident radiation in solar pond

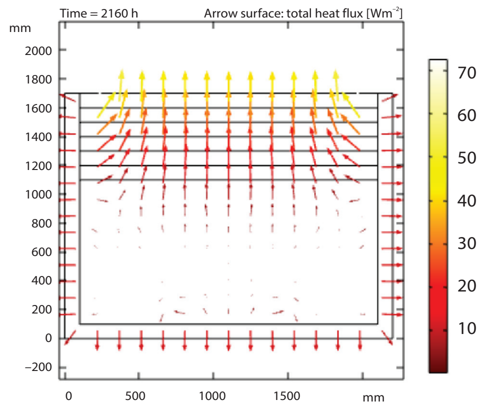

Figure 3. Total heat flux out of surface of solar pond

Table 1. Computational conditions

Ambient temperature	293.15 K
Ambient pressure	1 atm
Radiation discretization Method	Discrete ordinate
Discrete ordinate	S4
Performance index	0.4
Wall type	Gray
Insulation	Foam

Table 2. The solar radiation and temperature data for Adana

	Jan.	Feb.	Mar.	Apr.	May	June	July	Aug.	Sept.	Oct.	Nov.	Dec.
Temperature [ºC]	9.4	10.4	13.3	17.3	21.6	25.5	28.0	28.4	25.8	21.2	15.5	11.0
Solar radiation [Wm^{-2} per day]	1980	2420	4120	4980	6070	6680	6460	5910	4900	3780	2330	1810
Soil temperature [K]	13.3	14.7	16.4	19.6	22.8	24.2	25.3	26.6	24.1	21.8	18.3	14.2

the surface of the pond is open and the highest heat loss was expected to be happened with the way of natural-convection. The heat flow out of the pond was simulated and is shown in fig. 3. Numerical calculation show that the highest heat flow was calculated out of the surface with by natural-convection. Since the side walls and the floor are equally insulated, the heat losses on these boards are as expected to be equal. The temperature distribution of the modeled solar pond and internal energy capacity distribution are given in fig. 4. The depth of HSZ in the solar pond is 100 cm and the maximum temperature was stabled at 322 K. The pond temperature did not increase after certain value and the loss and the gain were equalized with time. When fig. 4(a) is examined, there is a uniform temperature distribution in the storage zone due to the effect of insulation. However, temperature of the UCZ zone is almost equal to the outdoor temperature. On the other hand, in the NCZ region it varies from lowest to highest temperature in the solar pond and these two zone were simulated to be the region where highest heat losses happens due to natural-convection.

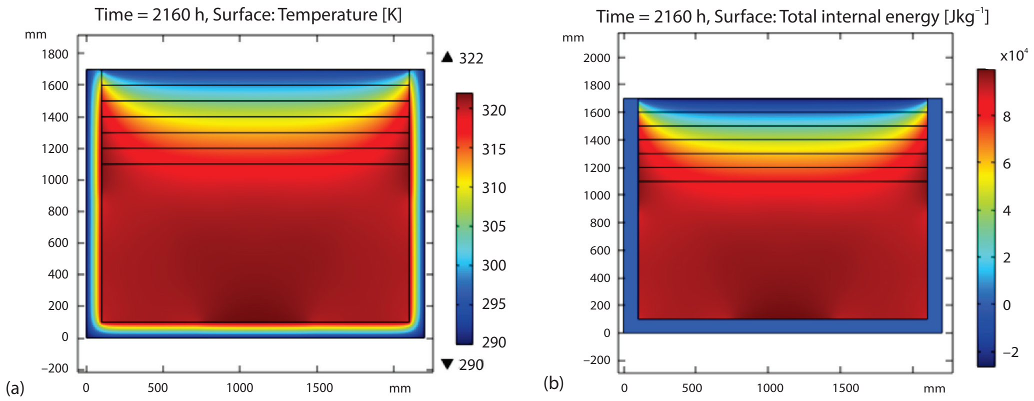

Figure 4. Temperature and total internal energy distribution in the solar pond; (a) temperature, (b) energy

In this part, the depth of the HSZ was increased from 40-400 cm, while the size and number of other layers were kept constant. In this section, 12 different solar ponds with varied depth were modeled and variation of temperature with respect to simulation time for five different points are given in fig. 5. The temperature data were calculated in the lower, middle and upper part of the HSZ, in the middle part of the NCZ and in the lower part of the UCZ. According to all the graphs in fig. 5, temperature first increased at the defined points then reached an equilibrium temperature and stayed constant at around 322 K. However, time to reach equilibrium temperature increases together with dept. The solar pond, which is 40 cm deep in the HSZ, reaches equilibrium temperature at around 1000 hours. The time increases as the depth increases and the deepest pond reaches the equilibrium temperature at the end of 6000 hours. There is a slight decrease in temperature after reaching the equilibri-

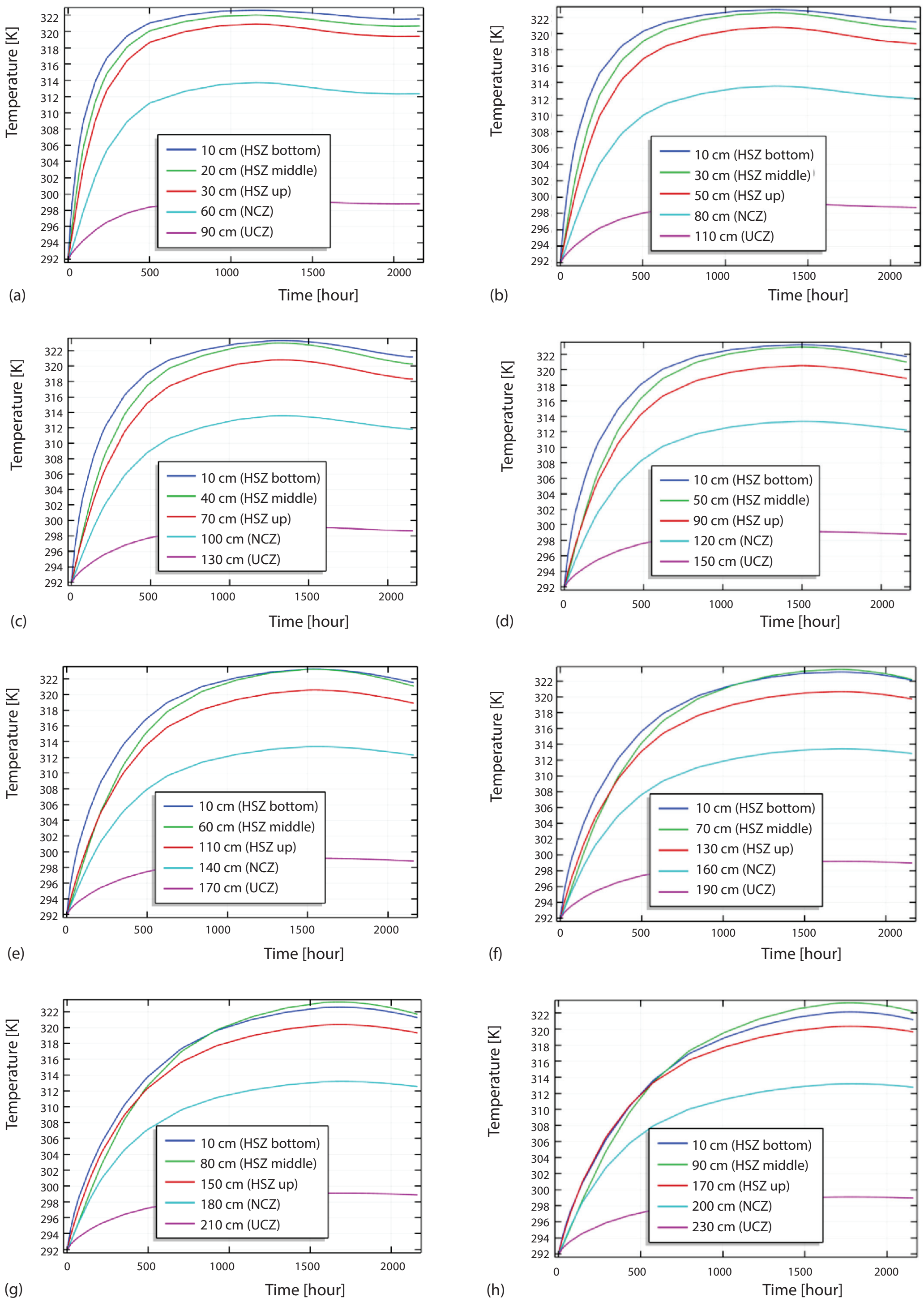
Temperature [K]
Time [hour]
(a)
10 cm (HSZ bottom)
20 cm (HSZ middle)
30 cm (HSZ up)
60 cm (NCZ)
90 cm (UCZ)
(b)
10 cm (HSZ bottom)
30 cm (HSZ middle)
50 cm (HSZ up)
80 cm (NCZ)
110 cm (UCZ)
(c)
10 cm (HSZ bottom)
40 cm (HSZ middle)
70 cm (HSZ up)
100 cm (NCZ)
130 cm (UCZ)
(d)
10 cm (HSZ bottom)
50 cm (HSZ middle)
90 cm (HSZ up)
120 cm (NCZ)
150 cm (UCZ)
(e)
10 cm (HSZ bottom)
60 cm (HSZ middle)
110 cm (HSZ up)
140 cm (NCZ)
170 cm (UCZ)
(f)
10 cm (HSZ bottom)
70 cm (HSZ middle)
130 cm (HSZ up)
160 cm (NCZ)
190 cm (UCZ)
(g)
10 cm (HSZ bottom)
80 cm (HSZ middle)
150 cm (HSZ up)
180 cm (NCZ)
210 cm (UCZ)
(h)
10 cm (HSZ bottom)
90 cm (HSZ middle)
170 cm (HSZ up)
200 cm (NCZ)
230 cm (UCZ)

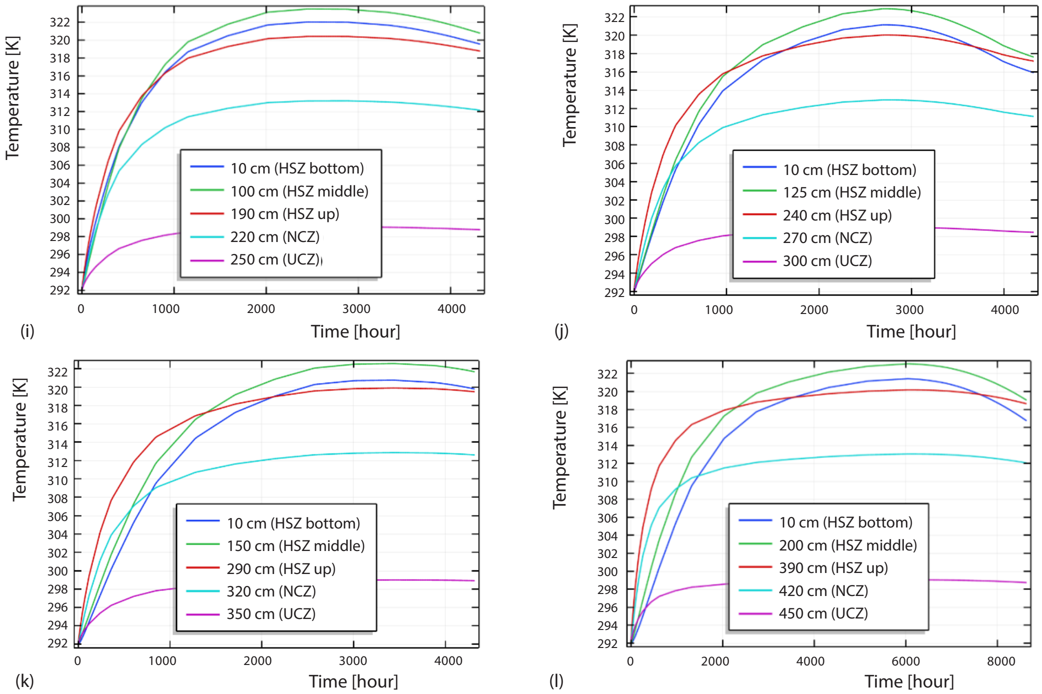

Figure 5. Duration of saturation temperature for varied depths of HSZ in solar pond; (a) 40 cm, (b) 60 cm, (c) 80 cm, (d) 100 cm, (e) 120 cm, (f) 140 cm, (g) 160 cm, (h) 180 cm, (i) 200 cm, (j) 250 cm, (k) 300 cm, and (l) 400 cm

um as shown in fig. 5. This is because the maximum temperature does not actually decrease but only the maximum temperature region is replaced as the simulation time increases. When the HSZ temperature curves are examined, there is a noticeable temperature differences in the lower, middle and upper parts of the HSZ, and as the depth increases, there is a homogeneous temperature distribution for the lower and middle parts in the HSZ. In all calculations, the average temperature of the HSZ was remained constant at around 45 °C. In the NCZ, there is a temperature distribution between the lowest and the highest temperature value in the pond. The temperature of the UCZ zone is around 25 °C, which is equal to the average temperature of the air. For a depth of 40 cm, the equilibrium temperature was reached in 1000 hours, 1300 hours for 60 cm, 1400 hours for 80 cm, 1500 hours for 100 cm, 1600 hours for 120 cm, 1750 hours for 1140 cm, 1800 hours for 180 cm, 2700 hours for 200 cm, 1800 hours for 250 cm, 3400 hours for 300 cm, and 6000 hours have passed for 400 cm. As the depth increases, time to reach to the equilibrium temperature increases but increment of amount of water and time to reach equilibrium temperature shows a proportional increase. If the stored heat wants to be used immediately, the storage area should be constructed shallow, but if the heat want to be used after certain times then deeper solar pond can be built.

In addition, the effect of the solar pond width on equilibrium temperature and time to reach maximum point was investigated without considering shadowing effect. For this, solar pond width was increased starting from 2-100 m by keeping depth constant and calculated data are given in fig. 6. It is seen that the equilibrium temperature differs slightly as the width of the pond increases. The main reason for this situation is that the heat stored in the middle part of the solar pond is moved away from the side walls and due to this, conduction losses are lower.

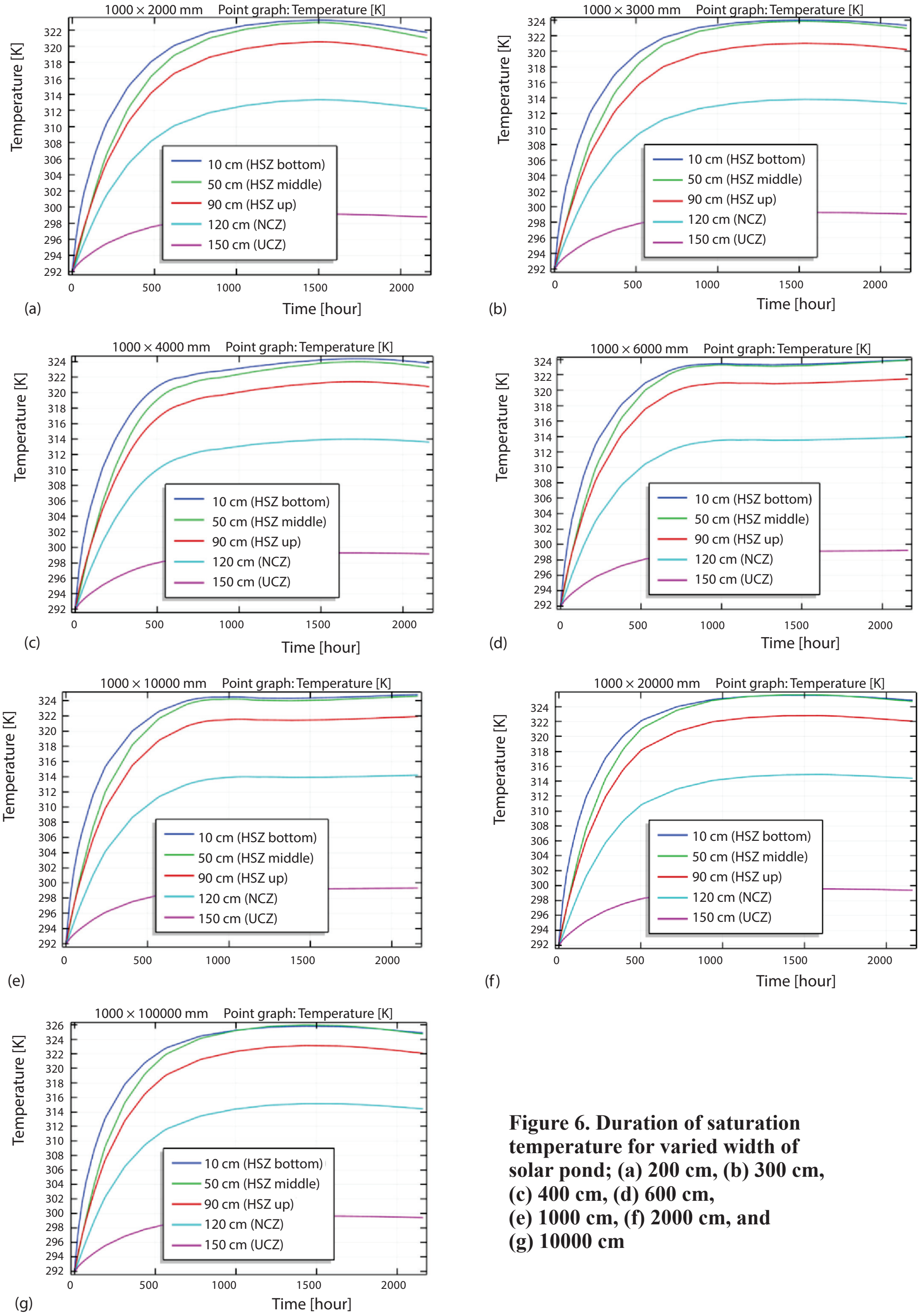

Figure 6. Duration of saturation temperature for varied width of solar pond; (a) 200 cm, (b) 300 cm, (c) 400 cm, (d) 600 cm, (e) 1000 cm, (f) 2000 cm, and (g) 10000 cm

In addition, as the width increases, the air contact with the surface also increases in parallel and natural-convection losses on the surface remain constant. If there was a change for the heat loss by natural-convection, there would be remarkable differences in the equilibrium temperature but as seen in the fig. 6, maximum temperature changed from 1-2 °C.

Conclusion

Solar pond is a system where solar energy is stored as heat energy at low and medium temperature. These systems reach the maximum saturation temperature after a certain time depending on the solar energy incoming to the surface. After reaching saturation temperature, the incoming solar energy balances heat losses out of the system and consequently no change in the temperature of the system is observed. In this study, the saturation temperatures and times period of solar pond were determined according to the size of different storage areas and incoming solar energy. Likewise, in the second part, the depth of the pond was kept constant and the width was increased. In this case calculations show that when the pond width is increased the solar energy coming to the surface of the pond increases and also increase of the mass of the salt water forming the pond indicating that there is no change for the saturation temperature and time. As a result, the saturation temperature and time give us information about when the heat should be pulled out of the pond. Using the heat from the system that reaches the saturation temperature will enable the temperature of the system to rise again with the later incoming solar energy. This lead a significant improvement in the performance of the system.

Acknowledgment

Many thanks to Middle East Technical University and Adiyaman University for technical support.

Nomenclature

C_p – specific heat capacity at constant pressure, [Jkg^{-1}K^{-1}]
$I(\Omega)$ – radiative intensity at a given position following the Ω direction, [Wm^{-2}s^{-1}r^{-1}]
$I_b(T)$ – blackbody radiative intensity, [Wm^{-2}s^{-1}r^{-1}]
Nr – refractive index (dimensionless)
$\vec{n}$ – outward normal vector (dimensionless)
Q – heat sources other than viscous heating, [Wm^{-3}]
$\vec{q}$ – heat flux by conduction, [Wm^{-2}]
$\vec{q}_r$ – heat flux striking the wall, [Wm^{-3}]
$\mathbf{S}$ – Strain-rate tensor, [s^{-1}]
T – absolute temperature, [K]
t – time, [s]
$\vec{u}$ – velocity vector, [ms^{-1}]

Greek symbols

α – coefficient of thermal expansion
β – extinction coefficients, [m^{-1}]
κ – absorption coefficients, [m^{-1}]
ρ – density, [kgm^{-3}]
σ – Stefan-Boltzmann constant, [JK^{-1}]
σ_s – scattering coefficients, [m^{-1}]
$\varphi(\Omega', \Omega)$ – scattering phase function (dimensionless)

References

[1] Chekerovska, M., Filkoski R. V., Efficiency of Liquid Flat-Plate Solar Energy Collector with Solar Tracking System, *Thermal Science*, *19* (2015), 5, pp. 1673-1684
[2] Bozkurt, I., *et al*., An Investigation of the Effect of Transparent Covers Effect on the Performance of a Cylindrical Solar Pond, *International Journal of Green Energy*, *11* (2014), 4, pp. 404-416
[3] Bezir, N. C., *et al*., Numerical and Experimental Analysis of a Salt Gradient Solar Pond Performance with or without Reflective Covered Surface, *Applied Energy*, *85* (2008), 11, pp. 1102-1112
[4] Bozkurt, I., *et al*., Modelling of a Solar Pond for Different Insulation Materials to Calculate Temperature Distribution, *Journal of Multidisciplinary Engineering Science and Technology*, *2* (2015), 6, pp. 1378-1382

[5] Karakilcik, M., *et al*., Dynamic Exergetic Performance Assessment of an Integrated Solar Pond, *International Journal of Exergy*, *12* (2013), 1, pp. 70-86
[6] Bozkurt, I., Karakilcik, M., The Daily Performance of a Solar Pond Integrated with Solar Collectors, *Solar Energy*, *86* (2012), 5, pp. 1611-1620
[7] Sogukpinar, H., *et al*., Numerical Evaluation of the Performance Increase for a Solar Pond With Glazed and Unglazed, *Proceedings*, IEEE International Conference on Power and Renewable Energy, Melaka, Malaysia, 2016, pp. 598-601
[8] Bozkurt, I., Karakilcik, M., The Effect of Sunny Area Ratios on the Thermal Performance of Solar Ponds, *Energy Conversion and Management*, *91* (2015), Feb., pp. 323-332
[9] Bozkurt, I., *et al*., Performance Assessment of a Magnesium Chloride Saturated Solar Pond, *Renewable Energy*, *78* (2015), June, pp. 35-41
[10] Ganguly, S., *et al*., Investigation of Thermal Performance of a Solar Pond With External Heat Addition, *Journal of Solar Energy Engineering*, *140* (2018), 2, pp. 024501-0245507
[11] Sayer, A. H., *et al*., Behaviour of a Salinity Gradient Solar Pond during Two Years and the Impact of Zonal Thickness Variation on Its Performance, *Applied Thermal Engineering*, *130* (2018), Feb., pp. 1191-1198
[12] Akrour, D., *et al*., A Theoretical and Numerical Study of Thermosolutal Convection: Stability of a Salinity Gradient Solar Pond, *Thermal Science*, *15* (2011), 1, pp. 67-80
[13] Alcaraza, M., *et al*., Thermal Performance of 500 m^2 Salinity Gradient Solar Pond in Granada, Spain under Strong Weather Conditions, *Solar Energy*, *171* (2018), Sept., pp. 223-228
[14] Sayer, A. H., New Comprehensive Investigation on the Feasibility of the Gel Solar Pond, and a Comparison with the Salinity Gradient Solar Pond, *Applied Thermal Engineering*, *130* (2018), Feb., pp. 672-683
[15] Montala, M., *et al*., Stability Analysis of an Industrial Salinity Gradient Solar Pond, *Solar Energy*, *180* (2019), Mar., pp. 216-225
[16] Sogukpinar, H., *et al.*, Performance Comparison of Aboveground and Underground Solar Ponds, *Thermal Science*, *22* (2018), 2, pp. 953-961
[17] ***, Heat Transfer Module, COMSOL. https://www.comsol.com/[accessed 10 March 2018]
[18] Modest, M. F., *Radiative Heat Transfer*, 2nd ed., Academic Press, San Diego, Cal., USA, 2003
[19] Maugin, G. A., *The Thermomechanics of Non-Linear Irreversible Behaviors*: *An Introduction*, World Scientific, Singapore, 1999
[20] Incropera, F. P., *et al*., Fundamentals of Heat and Mass Transfer, 6th ed., John Wiley and Sons, New York, USA, 2006
[21] Karakilcik, M., *et al*., Performance Investigation of a Solar Pond, *Applied Thermal Engineering*, *26* (2006), 7, pp. 727-735
[22] Kayali, R., *et al.*, A Rectangular Solar Pond Model Incorporating Empirical Functions for Air and Soil Temperatures, *Solar Energy*, *63* (1998), 6, pp. 345-353

Paper submitted: December 12, 2018
Paper revised: April 2, 2019
Paper accepted: April 22, 2019